JOURNAL OF ENERGY, MATERIAL, AND INSTRUMENTATION TECHNOLOGY

Journal Webpage https://jemit.fmipa.unila.ac.id/

Extraction of Nanocellulose from Softwood Pine (*Pinus merkusii*) using Acid Hydrolysis Method

Anisyah Anggraini*, Posman Manurung, Sri Wahyu Suciyati, and Yanti Yulianti

Department of Physics, University of Lampung, Bandar Lampung, Indonesia, 35141

Article Information

Article history:
Received November 17, 2022
Received in revised form November 25, 2022
Accepted November 2, 2023

Keywords: *nanocellulose, pine, hydrolysis method, H_2SO_4*

Abstract

Extraction of softwood pine (Pinus merkusii) as the main ingredient for the manufacture of nanocellulose was carried out through the acid hydrolysis method. In this research, four samples were made with varying concentrations of H_2SO_4. The samples that have been made have been tested by X-ray diffraction (XRD), Scanning Electron Microscopy (SEM), and Fourier Transformed Infrared (FTIR). XRD diffractograms were analyzed qualitatively and quantitatively. XRD analysis shows that the greater the concentration of H_2SO_4 used, the percentage of purity of each sample increases. The phase identification results show that the samples with the addition of 19, 29, and 39% H_2SO_4 form I_α, I_β, and lignin phases. While in the sample with the addition of 45% H_2SO_4, only I_α and I_β phases are formed. Image identification from SEM test results shows that the image pattern has a distribution shape structure resembling a compact and overlapping arrangement of stone slabs. FTIR analysis shows the functional groups formed are O-H, C-H, C≡C, C=C, H-C-H, C-O, and C-O-C, which indicates the presence of cellulose.

Informasi Artikel

Proses artikel:
Diterima 17 November 2022
Diterima dan direvisi dari 25 November 2022
Accepted 2 November 2022

Kata kunci: *Nanoselulosa, Pinus, hidrolisis asam, H_2SO_4*

Abstrak

Telah dilakukan pembuatan nanoselulosa berbasis kayu lunak pinus (Pinus merkusii) menggunakan metode hidrolisis asam. Pada penelitian ini dibuat 4 sampel dengan variasi konsentrasi H_2SO_4. Sampel yang telah dibuat dilakukan uji X-Ray Diffraction (XRD), Scanning Electron microscopy (SEM) dan Fouried Transformed Infrared (FTIR). Difraktogram XRD dianalisis secara kualitatif dan kuantitatif. Analisis XRD merujuk bahwa semakin besar konsentrasi H_2SO_4 yang digunakan maka persentase kemurnian dari masing-masing sampel meningkat. Hasil identifikasi fasa diperoleh bahwa sampel dengan penambahan H_2SO_4 19, 29, dan 39% terbentuk fasa I_α, I_β dan lignin. Sementara, pada sampel dengan penambahan H_2SO_4 45% hanya terbentuk fasa I_α, dan I_β. Identifikasi gambar hasil uji SEM diperoleh bahwa pola gambar memiliki struktur bentuk distribusi menyerupai susunan lempengan batu yang rapat dan saling tumpang tindih. Analisis FTIR menunjukkan gugus fungsi yang terbentuk yaitu O-H, C-H, C≡C, C=C, H-C-H, C-O dan C-O-C yang menunjukkan kehadiran selulosa.

1. Introduction

Nanotechnology is increasingly attractive to various groups, both in industry and researchers. The advantage of nanotechnology is that it can produce samples with high mechanical strength, this is due to the large nanofiber ratio between the surface area and volume of the nanofiber so that the molecules become more reactive (Huang et al., 2003). The application of nanotechnology in manufacturing products based on natural resources (forests) is very promising for fundamental changes, new added value and tangible benefits, and more efficient use of renewable and non-renewable materials. The benefit of nanotechnology is to obtain nanomaterials. Among the many types of nanomaterials, there is an exciting plant-based material called nanocellulose. Using nanoscale cellulose (nanocellulose) in composites will produce materials lighter than current composites in various applications (Cowie et al., 2014).

Nanocellulose is a material made of cellulose that has a nano size with a diameter of about 1-100 nm and a length of 10-100 nm (Lee et al., 2014). Nanocellulose has advantages such as low density, high chemical reactivity,

* Corresponding author.
E-mail address: anisyah.anggraini001@gmail.com

high strength, and modulus. These properties make nanocellulose have potential with high utility value and can be used more widely. Recently, nanocellulose applications in high demand, such as fillers, nanocomposites, and paper production materials, and the medical field such as wound dressings, suspension stabilizers, disintegrating agents in solid pharmaceutical preparations such as tablets and capsules, and drug carriers to target cells and soft tissue implants (Xie et al., 2018). The use of nanofibers has been widely carried out, such as using the basic materials of pineapple leaf fiber, snake-fruit tree frond fiber, palm oil bunch fiber, kenaf fiber, cellulose from potato powder, and cellulose produced from Gluconacetobacter xylinu bacteria. In this study, the base material of soft pine wood (Pinus merkusii) was used to make cellulose nanocrystals.

Pine, belonging to the Pinaceae family, grows naturally in Aceh, North Sumatra, and Mount Kerinci (Khaerudin, 1999). The composition of pine wood contains (47.5%) cellulose, (29.9%) lignin, and (12%) other substances including sugar. Based on its cellulose content, pine has the potential as a source of cellulose that can be used in the manufacture of nanocellulose to produce a final product that has a high sales value and is expected to be able to reduce wood waste (Octaviana, 2016). A widely used method in the extraction of nanocellulose is the chemical method with acid hydrolysis. Hydrolysis using sulfuric acid makes cellulose negatively charged on its surface due to cellulose sulfate (Klemm et al., 1998). The greater the concentration of sulfuric acid used, the greater the charged groups on nanocellulose, but if the concentration is too great, it will reduce its crystallization (Lee et al., 2014).

In this research, it will be proposed to extract nanocellulose from softwood pine (Pinus merkusii) using the acid hydrolysis method and then analyze the microstructure and phases produced by each sample. The prepared samples will be characterized using X-ray diffraction (XRD) to determine the lattice structure, degree of crystallinity, and particle size, as well as Fourier Transformed Infrared (FTIR) to determine the functional groups formed and Scanning Electron Microscopy (SEM) to determine the morphological structure.

2. Research Methods

This research begins by preparing the tools and materials that will be used. After that, the remaining pine wood is bleached using textile bleach), then dried in the sun. Then, continue to the pre-treatment/ delignification stage, at this stage 10 grams of pine wood waste is mixed with 100 ml NaOH 3% and then stirred using a covered hot plate at a temperature of 50ºC for 2 hours. The delignification process aims to remove the lignin content in pine wood waste.

After going through the delignification process, the next step is to enter the acid hydrolysis stage. At the acid hydrolysis stage, 10 grams of pine wood waste resulting from the delignification process was mixed with 100 ml of various concentrations of H_2SO_4 19, 29, 39 and 45% and then stirred while being heated using a hot plate at a temperature of 45ºC for 1 hour. This stage removes the remaining hemicellulose and lignin content in pine wood waste. The result of the hydrolysis process of the sample is in the form of pre-cellulose Nano Crystals (p-CNC), which are then washed with 300 ml of aquabides. After washing, p-CNC was centrifuged for 10 min for three replicates.

After the p-CNC is centrifuged, drop the p-CNC with 10% NaOH solution to neutral pH (pH = 7), then filter the p-CNC using filter paper. The next step is drying using an oven at a temperature of 100ºC for 30 minutes periodically to obtain CNC, which is then ground using a mortar to form a powder.

CNC samples in powder form are required to facilitate the characterization process. To find out the physical characterization results of each CNC sample variant, XRD, FTIR, and SEM characterization were carried out.

3. Results and Discussions

The results of synthesizing pine wood waste through the acid hydrolysis process in the form of CNC powder are shown in **Figure 1.**

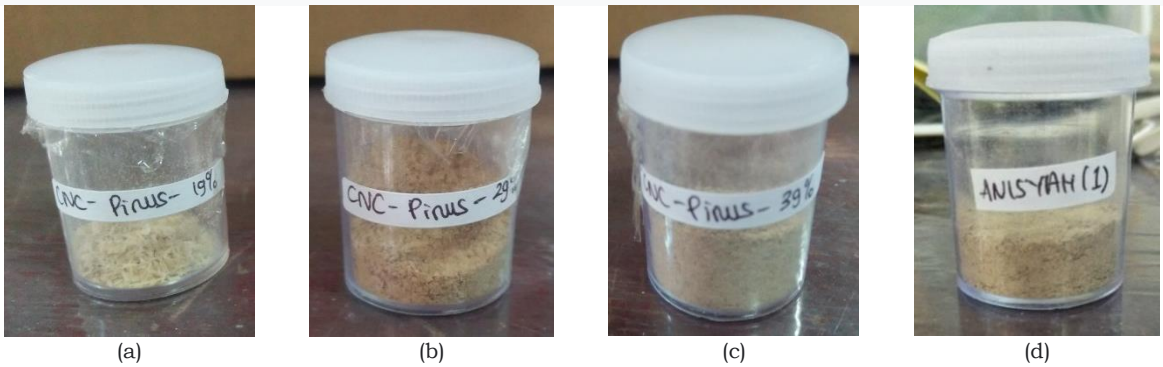

(a) (b) (c) (d)

Figure 1. CNC resulting from the hydrolysis of H_2SO_4 (a) 19%, (b) 29%, (c) 39%, and (d) 45%

Based on **Figure 1**, it can be seen that there is a significant difference in physical characteristics in the form of the color of CNC samples based on the variation in the concentration of H_2SO_4 used. The CNC-19% sample has the lightest color compared to the other CNC samples, while the CNC-45% sample has the darkest relative color compared to the other CNC samples. It can happen because of the influence of variation in the concentration of H_2SO_4 used. The higher the concentration of H_2SO_4 used, the color of the CNC sample tends to be due to cellulose degradation, dehydration, and cellulose carbonation. This is because the acid can penetrate quickly into the cellulosic tissue layer and participate in hydrolyzing the amorphous region. The cellulose itself is easily soluble in strong acids (high concentration). In addition, sulfuric acid is a strong oxidizing agent, causing a powerful reaction with water and causing high heat (Loelovich, 2012).

3.1 XRD Analysis

1. Qualitative Analysis

Qualitative analysis was used to determine the crystallinity by observing the XRD test results in the form of crystalline intensity (I_{max}) in the range of 2θ 20-23° and amorphous intensity (I_{am}) in the range of 2θ 18-19°. Furthermore, the relationship between peak intensity and diffraction angle 2θ was then made into a diffractogram, as shown in **Figure 2.**

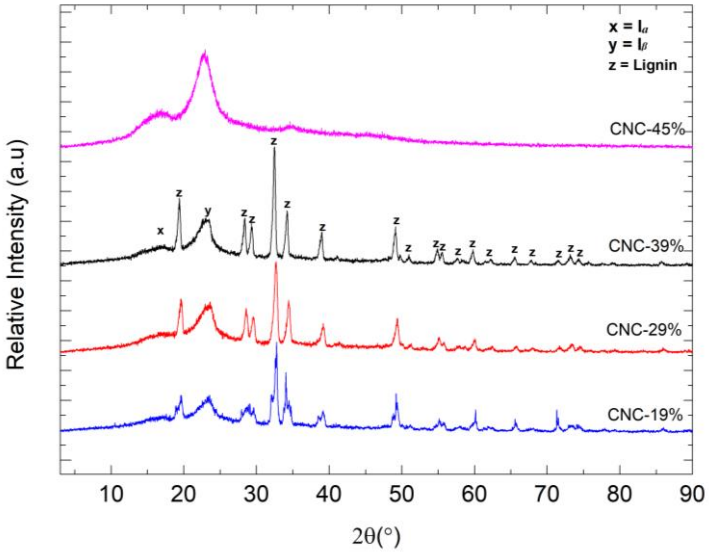

Figure 2. Diffractogram of XRD test results of pine softwood nanocellulose

Figure 2 shows the diffractogram results of nanocellulose samples extracted from pine wood waste. Based on the XRD test results of CNC-19%, CNC-29%, and CNC-39%, samples show more than two diffraction peaks that identify the impurity phase. Meanwhile, the exact shape of the nanocellulose diffractogram is illustrated by the CNC-45% sample. The CNC-45% sample shows exactly two diffraction peaks. It shows the presence of crystalline phases I_{β} (first maximum peak) and I_{α} (second maximum peak) corresponding. It can be reconciled with previous research on soft wood-based nanocellulose conducted by Wei Li *et al.* (2011) and Trisanti *et al.* (2018).

To determine the degree of crystallinity (I_c) of each sample, it can be done by calculating the diffraction peak intensity (I_{max} and I_{am}) based on Segal's formula**:**

$$I_C = \frac{I_{max} - I_{am}}{I_{max}} \times 100\% \quad (1)$$

Whose results are shown in **Table 1.**

Table 1. CNC crystallinity index calculation results

Sample	$2\theta_{max}$ (°)	I_{max} (cps)	$2\theta_{am}$ (°)	I_{am} (cps)	I_c (%)
CNC-19%	23.36	367	18.3	177	51.77
CNC-29%	23.53	516	18.1	227	56.78
CNC-39%	23.32	387	17.9	165	57.36
CNC-45%	23.01	914	18.3	342	62.58

Table 1 shows the increase in the degree of crystallinity in four CNC pine samples, namely CNC-19% by 51.77%, CNC-29% by 56.78%, CNC-39% by 57.36%, and CNC-45% by 62.58% which is directly proportional to the increased variance of H_2SO_4 concentration. The results of the XRD analysis can also be used to determine the CNC crystal size by analyzing the diffraction peak position of the crystal phase I_{β} from the XRD test data using Equation *Scherrer*:

$$L = \frac{K\lambda}{B\cos\theta} \quad (2)$$

The crystal size obtained from the I_{β} crystal phase can be seen in **Table 2**.

Table 2. CNC particle size calculation

Sample	K	2θ (°)	θ (°)	λ (nm)	FWHM (rad)	L (nm)
CNC-19%	0.9	23.36	11.68	0.15405	0.0357	3.9
CNC-29%	0.9	23.53	11.76	0.15405	0.0359	3.9
CNC-39%	0.9	23.32	11.66	0.15405	0.0342	4.1
CNC-45%	0.9	23.01	11.50	0.15405	0.0458	3

The CNC crystallite size in **Table 2** ranges from 3-4 nm. The result was that the largest particle size was obtained in the CNC-39% sample, which was 4,1 nm, and the smallest particle size was obtained in the CNC-45% sample, which was 3 nm. This value is consistent with a previous study by Wei Li *et al.* (2011), which produced a CNC particle size between 3-5 nm.

2. Quantitative Analysis

Quantitative analysis is done through data refinement with the Rietveld method. This Rietveld method provides a solution for studying phase changes (Mukminin, 2018). There are two types of phase purification calculation methods, namely Normal and Le Bail. The Normal method provides complete data with the molarity and weight of each phase but is more complicated because it must include atomic position values. In comparison, the Le Bail method does not include the atomic position value. The crystal data used as input is the Inorganic Crystal Structure Database (ICSD) database model for the ICSD database model used is the model of Nishiyama *et al.* (2003) with the chemical formula $C_{12}H_{20}O_{10}$, triclinic cell, space group P1, and Number The Crystallography Open Database (COD) is 00-411-4994, for phase Iα and the model of Nishiyama *et al., (*2002) with chemical formula $C_{12}H_{20}O_{10}$, monoclinic cell, space group P21, and the COD number is 00-411-4382 for phase I_{β}. The use of the ICSD database model is also due to the limitations of the phase smoothing calculation method. Furthermore, the results of XRD data purification of pine CNC samples were obtained, as shown in **Figure 3.**

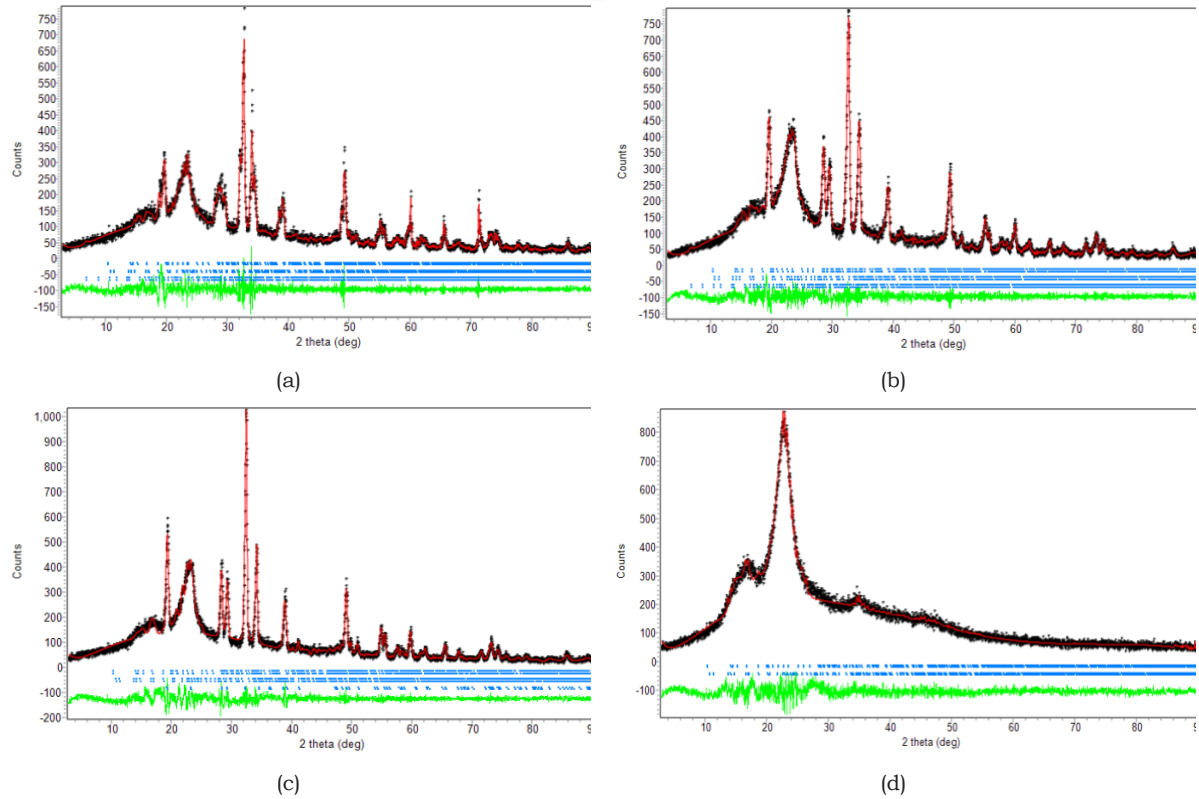

Figure 3. XRD CNC pine wood refining results (a) CNC-19%, (b) CNC-29%, (c) CNC-39% and (d) CNC-45%

Figure 3 shows the XRD data filtering diffractogram of four CNC samples undergoing crystal structure data refinement. In refining the diffractogram, the Rietveld method is used, paying attention to the Goodness of Fit (*GoF*) value sometimes denoted by 2. Ideally, the *GoF* price should be 1. It can happen when the price of the weighting factor and the expected factor get almost the same price. So when squared, it will give a number close to one. At the same time, a good *GoF* value should be less than 4 for phase analysis calculations (Kisi, 1994). In addition, the suitability of the purification output is shown through the values of R_p, R_{wp}, and R_{epx}. R_p is the R profile factor value whose value will decrease if the difference between the observed and calculated data intensities or the model used becomes smaller. R_{wp} is the weighted profile factor, and Rex is the expected R profile factor. The value of R_p, R_{wp}, and R_{exp} should be less than 20.

The results of the XRD data purification output can be used to determine the variation in the four-phase content composition of CNC samples. Iα is formed at a 2θ angle between 16-18° and has a triclinic structure. Meanwhile, I_{β}

is formed at an angle of 22-23° and has a monoclinic structure (Attala *et al.,* 1984). I_α can be formed naturally in cellulose molecules and degraded using hydrolysis methods to become more stable in the I_β form. The phase composition in molar percent contained in the pine CNC sample can be seen in **Table 3**.

Table 3. CNC phase parameters in molar percent (%M)

Sample	I_α (%M)	I_β(%M)	Lignin (%M)
CNC-19%	3.75 ± 0.00	14.82 ± 0,00	81.42 ± 0.01
CNC-29%	3.75 ± 0.00	14.83 ± 0,00	81.42 ± 0.01
CNC-39%	4.68 ± 0.00	18.45 ± 0.02	76.86 ± 0.10
CNC-45%	20.12 ± 0.00	79.88 ± 0.00	-

Based on **Table 3**, it can be seen that only the CNC-45% sample meets the requirements of CNC with two crystal phases in the form of I_α and I_β ($C_{12}H_{20}O_{10}$). Samples CNC-19%, CNC-29%, and CNC-39% contain an amorphous lignin phase ($C_{12}H_{20}O_{10}$) with a reasonably dominant amount. It can happen because the concentration of the NaOH solution used in the delignification stage is insufficient to hydrolyze the amorphous phase of lignin contained in the pine wood waste.

XRD data analysis produces output as improvements to the crystal structure based on the calculated diffraction pattern (Model). The following **Table 4-5** shows a comparison of CNC-45% cell parameters of the smoothing results to the model along with the percentage shift in the measurement value (MV)

Table 4. I_α phase CNC cell parameter of CNC-45%

Sample	a (Å)	b (Å)	c (Å)	α (°)	β (°)	γ (°)
Model	6.717	5.962	10.400	118.08	114.80	80.37
CNC-45%	6.682	5.961	10.390	118.06	114.68	80.41
MV (%)	0.26	0.03	0.06	0.05	0.04	0.08

Based on **Table 4**, the calculation result obtained from the measurement value shift in each phase of the Iα CNC cell parameter is less than 1%. Therefore, it can be concluded that the smoothing of the XRD data of the CNC-45% sample produced cell parameters of the I_α phase whose values correspond to the model of Nishiyama *et al.* (2003).

Table 5. I_β phase CNC cell parameter of CNC-45%

Sample	a (Å)	b (Å)	c (Å)	α (°)	γ (°)
Model	7.784	8.201	10.380	90.00	96.50
CNC-45%	7.784	8.201	10.379	90.00	96.50
MV (%)	0.000	0.000	0.609	0.00	0.00

Based on **Table 5**, the calculation results obtained from the measurement value shift occurring in each phase parameter I_β of the CNC cell is less than 1%. Therefore, it can be concluded that the smoothing of the XRD data of the CNC-45% sample results in cell parameters I_β of the phase whose values are in accordance with the model of Nishiyama *et al.* (2002).

3.2 SEM Analysis

SEM characterization was carried out to determine the surface morphology of the samples. SEM test was conducted on the best sample, which is CNC-45%. Samples were tested at a magnification of 10.000 times. The characterization results obtained are in the form of particle surface morphology, as can be seen in **Figure 4.**

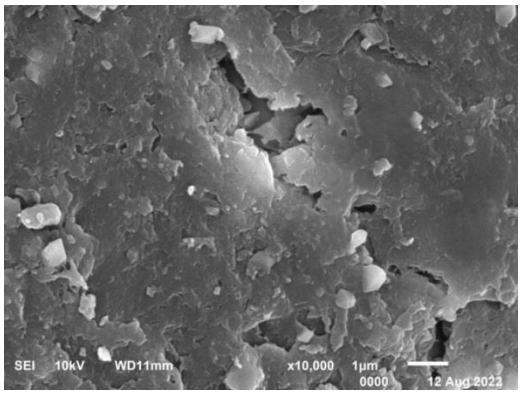

Figure 4 SEM test CNC-45%

Figure 4 shows the morphology of the SEM test results for the CNC-45% sample, which is relatively similar to the morphology of sengon wood (Trisanti *et al.,* 2018). SEM test results show that the grain distribution structure is

similar to a compact and overlapping arrangement of stone slabs. It makes it difficult to measure the distribution of nanocellulose particles and makes I_a and I_β phase particles challenging to distinguish from each other.

3.3 FTIR Analysis

FTIR characterization in this study was conducted to identify the functional groups contained in the CNC sample by displaying the results in the form of a spectrum that expresses the relationship between the transmission of the IR spectrum and the wave number in the sample. The wavenumber range used is 4.000 cm^{-1} to 650 cm^{-1} with a resolution of 16 cm^{-1}. The following FTIR results from CNC samples are shown in **Figure 5.**

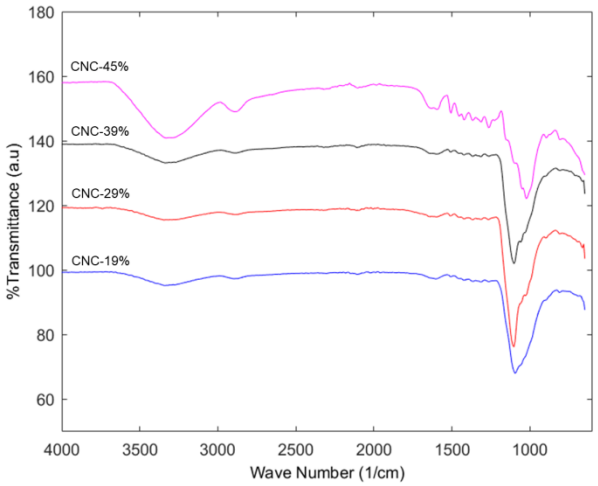

Figure 5 FTIR Spectra CNC

Figure 5 is the overall result of FTIR analysis for CNC-19%, CNC-29%, CNC-39% and CNC-45% samples. From the entire CNC sample, the results of functional group analysis, vibration type, and bond intensity were obtained, which refer to the IR absorption table (Libretexts, 2022) as shown in **Table 6.**

Table 6. Results of FTIR spectrum analysis of CNC samples

CNC-19%	CNC-29%	CNC-39%	CNC-45%	Functional Groups	Type of Vibration	Intensity
3339	3347	3339	3332	O-H	Stretching	Strong
2892	2892	2892	2892	C-H	Stretching	Medium
-	-	2109	2102	C≡C	Stretching	Weak
1602	1595	1595	1595	C=C	Stretching	Medium
1423	1423	1423	1423	H-C-H	Bending	Medium
-	-	-	1371	O-H	Bending	Medium
1312	-	1312	-	C-O	Stretching	Strong
-	1103	1103	-	C-O-C	Stretching	Strong
1095	-	-	1021	C-O	Stretching	Strong

Table 6 is the overall result of the FTIR analysis on each CNC-19%, CNC-29%, CNC-39%, and CNC-45% samples that do not show significant differences and have the same functional group detected. It is evidenced by the peak wave number found in each FTIR spectrum. In cellulose, the absorption area between 3332-3347 cm^{-1} shows that the entire FTIR spectrum with the leading O-H bond group shows that in each CNC sample, there is still water content that shows the hydroxyl group (Lusiana, 2019) in addition to the peak wave number 3332 cm^{-1} is characteristic stretching of hydroxyl groups in polysaccharides which also includes inter- and intra-molecular hydrogen vibrations in cellulose. Removing the water content in cellulose is quite tricky; this is due to the interaction between cellulose and water due to inter and intra-molecular bonds in cellulose, which cause this band to remain even after going through the acid hydrolysis process. The chemical bonds formed are generally single and vibrate in a strong to medium-intensity stretch. Cellulose was also detected at a wave number of 2892 cm^{-1}, which indicates C-H functional groups in each CNC sample, which are aliphatic in cellulose, hemicellulose, and lignin (Sain et al., 2006).

In the wavenumber region 1500-600 cm^{-1}, to determine the content of a particular compound, the identification of functional groups can be carried out. The functional group detected is usually CH_2, which has a moderate-intensity bending vibration resulting from the deformation of the C-H group detected in four CNC samples (Jonoobi et al.,

2009). The wave number regions of 1312, 1095, and 1021 cm^{-1} with C-O stretching groups are C-O glycosidic groups. Changes in cellulose structure due to variations in NaOH are indicated by O-H stretching at wave number 1371 cm^{-1}. The peak wave number 1602-1595 cm^{-1} indicates C=C alkene from lignin and shows absorption from water due to strong interaction between cellulose and hydrophilic water with moderate stretching vibration (Johar et al., 2012). In CNC-39% and CNC-45% samples, there are alkyne functional groups in C≡C at wave numbers 2109 cm^{-1} and 2102 cm^{-1} with stretching vibrations of weak intensity. Seen in the CNC-45% spectrum, the peak intensity is sharper than the others, which indicates a better crystal structure than the CNC 19, 29 and 39% spectra.

Furthermore, the last group detected at the wave number 1103 cm-1 for CNC-29% and CNC-39% samples, which is the functional group C-O-C (pyranose ring). Pyranose is a ring structure consisting of 6 atoms formed due to the reaction of the hydroxyl functional group of the alcohol on the C5 atom with the aldehyde on the C1 atom, which vibrates in stretching with solid intensity. This group also shows an increase in the crystallinity of the CNC phase (Yang et al., 2021).

4. Conclusions

From the research that has been done, it can be concluded that XRD analysis shows that nanocellulose extracted from pine softwood has a purity level of 62.58% with crystal measuring 3 nm for the CNC-45% sample. In comparison, SEM analysis shows that the distribution of nanocellulose particles resembles the shape of a compact and overlapping stone slab arrangement, and FTIR analysis shows that the functional groups formed are O-H, C-H, C≡C, C=C, H-C-H, C-O, and C-O-C functional groups.

5. Bibliography

Attala, R. H. & Vanderhart, D. L. (1984). Native Cellulose: A Composite of Two Distinct Crystalline Forms. *Science*. Vol. 223. Hal. 283.

Cowie, J., Bilek, E. M., & Wegner, T. H. (2014). Projections of cellulose nanomaterial-enabled products-Part II. *TAPPI Journal*, Vol. 13, No.5, Hal. 9-16.

Huang, Z. M., Zhang, Y. Z., Kotaki, M., & Ramakrishna, S. (2003). A Review on Polymer Nanofibers by Electrospinning and Their Applications in Nanocomposites. *Composites Science and Technology*, No.63, Hal. 2223-2253.

Johar, N., Ahmad, I. & Dufresne, A. (2012). Extraction, Preparation and Characterization of Cellulose Fibres and Nanocrystas from Rice Husk. *Industrial Crops and Products*. Vol. 44, No. 22, Hal. 93-99.

Jonoobi, M., Harun, J., Shakeri, A., Misran, M. & Oksman, K. (2009). Chemical Composition, Crystallinity and Thermal Degradation of Bleached and Unbleached Kenaf Bast (*Hibiscus cannabius*) Pulp and Nanofibers. *BioRes*. Vol. 4, No. 2, Hal. 633-634.

Khaerudin. (1999). *Pembibitan Tanaman HTI*. Jakarta. Penebar Swadaya. Hal. 79–81.

Kisi, E. J. (1994). Rietveld Analysis of Powder Diffraction Patterns. *Materials Forum.* Hal. 135–153.

Klemm, D., Philipp, B., Heinze, T., Heinze, U., & Wagenknecht, W. (1998). *Functionalization of Cellulose.Weinheim. Wiley*-VCH Verlag GmbH. Comprehensive Cellulose Chemistry. Vol.2, Hal. 2-3.

Lee, H. V., Hamid, S. B. A., & Zain, S. K. (2014). Conversion of Lignocellulosic Biomass to Nanocellulose: Structure and Chemical Process. *Review Article. Scientific World Journal 2014*. Vol. 27, Hal. 631-639.

Libretexts. (2022). Infrared Spectroscopy Absorption Table. Hal. 1-4. https://chem.libretexts.org/@go/page/22645.

Loelovich, M. (2012). Optimal Conditions for Isolation of Nanocrystalline Cellulose particles. *Nanoscience and Nanotechnology*, Vol. 2, No. 2, Hal. 9-13.

Lusiana, S. E. (2019). Biocellulose Isolated from The Waste of Pinecone Flower (*Pinus merkusii Jungh Et De Vriese*). *Journal of Physics: Conference Series*. Vol. 10, No. 1, Hal. 6596-1742.

Mukminin, R. J., Martini, A., Nairn, J., Simonsen, J., & Youngblood, J. (2018). Cellulose nanomaterials review: Structure, properties and nanocomposites. *Chemical Society Reviews*, Vol. 40, No.7, Hal. 3941.

Nishiyama, Y., Langan, P., & Chanzy, H. (2002). Crystal Structure and Hydrogen-Bonding System in Cellulose I_{β} from Synchrotron X-ray and Neutron Fiber Diffraction. *American Chemical Society*. Vol. 124, No. 31, Hal. 9076.

Nishiyama, Y., Sugiyama, J., Chanzy, H., & Langan, P. (2003). Crystal Structure and Hydrogen-Bonding System in Cellulose I_{α} from Synchrotron X-ray and Neutron Fiber Diffraction. *American Chemical Society*. Vol. 125, No. 47, Hal. 14301.

Sain, M., & Panthapulakkal, S. (2006). Bioprocess Preparation of Wheat Straw Fibers and Their Characterization. *Industrial Crops and Products*. Vol. 23, Hal. 5.

Trisanti, P. N., Setiawan, S. H.P., Nura'ini, E., & Sumarno. (2018). Ekstraksi Selulosa dari Serbuk Gergaji Kayu Sengon melalui proses Delignifikasi Alkali Ultrasonik. *Jurnal Sains Materi Indonesia,* Vol. 19, No.3, Hal. 113-119.

Wei, L., Wang, R., & Liu, S. (2011). Nanocrystalline Cellulose Prepared from Softwood Kraft Pulp Via Ultrasonic-Assisted Acid Hydrolysis. *BioResources Journal*. Vol. 6, No.4, Hal. 4271-4281.